
Advanced Composite Materials
Publication details, including instructions for authors and subscription information:
http://www.tandfonline.com/loi/tacm20

# Development of Simulation Technology for Impact Behavior of CFRP/Al Alloy Hybrid Beams in Side Collision of Automobiles

Goichi Ben [a], Nao Sugimoto [b] & Yoshio Aoki [c]
[a] College of Industrial Technology, Nihon University, 1-2-1, Izumicho, Narashino, Chiba, 275-8575 Japan
[b] Presently with Honda Automobile Co., Japan
[c] College of Science and Technology, Nihon University, 7-24-1, Narashinodai Funabashi, Chiba, 274-8501 Japan
Version of record first published: 02 Apr 2012.

To cite this article: Goichi Ben , Nao Sugimoto & Yoshio Aoki (2010): Development of Simulation Technology for Impact Behavior of CFRP/Al Alloy Hybrid Beams in Side Collision of Automobiles, Advanced Composite Materials, 19:4, 363-379

To link to this article: http://dx.doi.org/10.1163/092430410X504152

VSP

*Advanced Composite Materials 19 (2010) 363–379*

ADVANCED COMPOSITE MATERIALS
brill.nl/acm

# Development of Simulation Technology for Impact Behavior of CFRP/Al Alloy Hybrid Beams in Side Collision of Automobiles

**Goichi Ben** [a,*], **Nao Sugimoto** [b] **and Yoshio Aoki** [c]

[a] College of Industrial Technology, Nihon University, 1-2-1, Izumicho, Narashino, Chiba, 275-8575 Japan

[b] Presently with Honda Automobile Co., Japan

[c] College of Science and Technology, Nihon University, 7-24-1, Narashinodai Funabashi, Chiba, 274-8501 Japan

Received 17 August 2009; accepted 5 October 2009



**Abstract**

Carbon fiber reinforced plastic (CFRP) laminates are used in various industrial fields because they have excellent properties in their specific strength and specific stiffness. The CFRP has a potential of weight reduction in the automotive structure, which can contribute to the improvement of mileage as well as the reduction of carbon dioxide. On the other hand, the safety issue in case of collision should be also clarified when employing the CFRP as automotive structures.

In this paper, hybrid beams which consisted of an Al alloy beam and a CFRP laminate were examined by both experiments and numerical analyses as candidates to replace the conventional steel door guarder beam used inside the automotive door. The experimental relations of impact loading to the displacement for the Al beams with different thicknesses, widths and types of CFRP showed good agreement with those from numerical results. In order to increase the impact energy absorption, other hybrid beams were devised and calculations performed by using the same parameters in the same numerical method and their results also agreed with those of experiments executed after the calculation. These facts show that the numerical method developed here can be generally used for estimating the impact behavior of CFRP/Al hybrid beams.

Furthermore, a suggestion for how to install the hybrid beam to automotive doors was proposed by the numerical method. As a result, the effectiveness of our simulation technology is demonstrated here.


**Keywords**

Impact, CFRP/Al hybrid beam, FEM, experiment, absorption energy

* To whom correspondence should be addressed. E-mail: ben.goichi@nihon-u.ac.jp
Edited by JSCM


DOI:10.1163/092430410X504152

## 1. Introduction

It is well known that $CO_2$ emitted from passenger vehicles is one of the major causes of global warming. The most effective method to reduce $CO_2$ is to produce fuel efficient automobiles. Improvement of the automobile fuel efficiency can be realized by reducing the automobile weight using a lightweight material for construction, such as composite materials. Carbon fiber reinforced plastics (CFRPs) have been widely used in aerospace industries, industrial goods and other application fields because of their high specific strength and high specific modulus compared with conventional metals. This means that CFRPs can contribute significantly to reducing the weight of automobiles.

Besides reducing the weight, the safety of automobiles is also a very important issue that needs to be investigated along with the reduction of weight. With increasing interests in reducing the automobile weight and securing the safety of passengers, extensive research has been performed in recent years into collision impact [1–6]. Collision safety of the automobile has been evaluated by full flap frontal crash, offset frontal crash and side impact tests. In the frontal crash, it is possible to absorb the energy by largely deforming the front and the rear parts of automobiles.

However, in the side crash, it is hard to absorb the impact energy in the same way as for the frontal crash, because the survival space of the passengers is very narrow. At present, door guarder beams made of steel are used inside the door to absorb the impact energy and their deformation is limited to about 150 mm.

In this study, we developed CFRP/Al hybrid beams as impact energy absorption members for side collision as shown in Fig. 1. Such members have the advantages of plastic deformation of aluminum alloy combined with high strength and lightweight of CFRP. By using the hybrid beam of aluminum alloy with the CFRP laminate, excellent energy absorption is expected within the limited deformation of 150 mm. The goal of this study is to develop simulation technology for the impact behavior of such hybrid members.

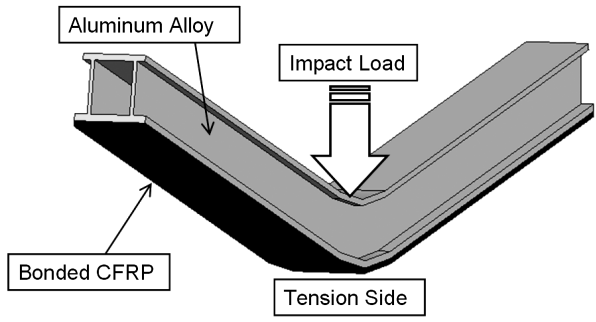


**Figure 1.** Bending deformation of hybrid beam.

## 2. Experimental

### 2.1. Specimens of the Hybrid Beam

An increase of impact energy absorption of Al beam with the CFRP laminate was examined in our previous paper [7]. When the thickness of CFRP laminate increased, the impact energy also increased, as shown in Fig. 2. The hybrid beam with 2.5 mm CFRP laminate absorbed 25% larger impact energy than that of the Al beam alone. The aluminum beam had the square section (30 × 30 mm), 3 mm thickness and was made of A7N01S-T5 with Young's modulus of 72 GPa, the yield stress of 312 MPa, and the tensile strength of 380 MPa. The CFRP of T700S and the high strength type of adhesive between the CFRP and the surface of aluminum alloy beam were used in the previous experiment. The impact test was executed by the same method as in this study (see Section 2.2) and the impact absorption energy was obtained from the area which was surrounded by the horizontal displacement axis and the curve of the impact load to the displacement at the center of beam.

In order to increase the impact absorption energy, the specimens of hybrid beams used in this study (Fig. 3) were different from the former one [7]. The aluminum alloy beam was of a stronger type (7000 series, Z6w-T5) than the previous one and it has Young's modulus of 70 GPa, the yield stress of 445 MPa, and the tensile strength of 480 MPa, and its cross-section shape was the unsymmetrical section to the horizontal axis as shown in Fig. 3. Three kinds of unidirectional CFRP laminate (T700, M40 and T800) and three types of adhesive (viscosity, high strength and high elongation) were used, respectively. Furthermore, the differences of the width (20, 28 and 36 mm) and the thickness (1, 2 and 3 mm) in the CFRP laminates were also employed. The effects of these design parameters on the impact energy absorption were examined by using the orthogonal table in the experimental design (Taguchi) method. Eighteen specimens with various combinations in the design parameters were fabricated and tested.

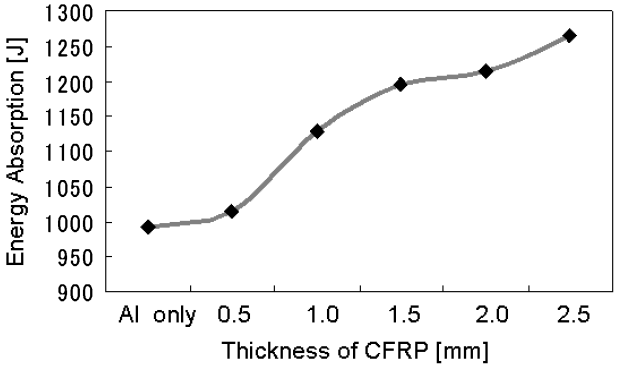


**Figure 2.** Increase of impact energy absorption.

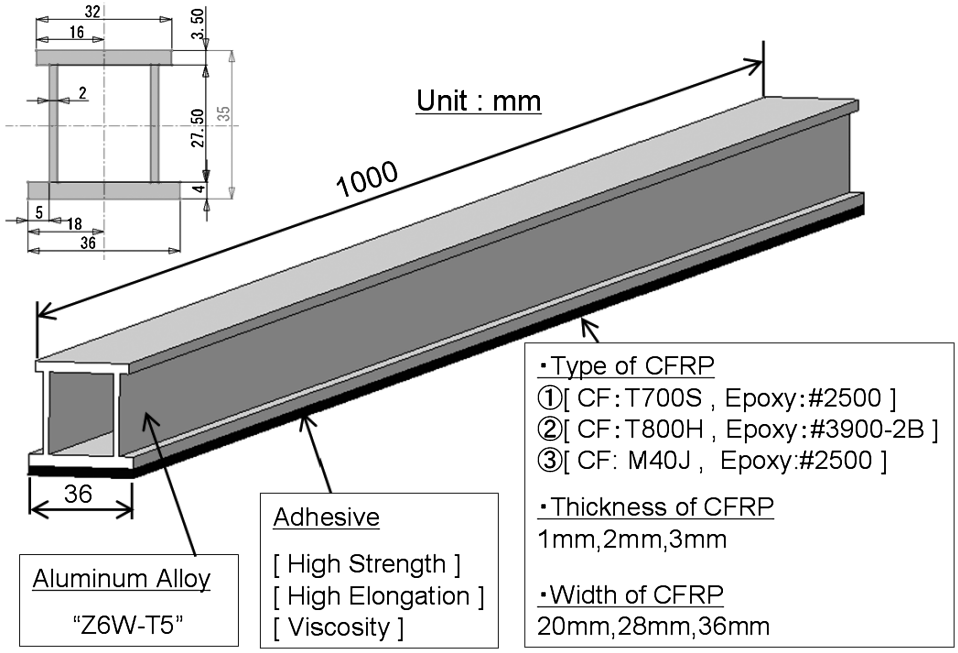


**Figure 3.** CFRP/Al hybrid beam.

### *2.2. Experimental Method*

The 1000 mm length of the hybrid beam was supported by two supporters having a head radius of 15 mm and the span between the two supporters was 800 mm. In order to evaluate the capacity of crash energy absorption, a larger size of drop tower facility for the impact test was constructed. The beam received an impact load generated by a free drop mass of 100 kg at an impact speed of 55 km/h. The shape of the impactor was a half cylinder having a 100 mm radius and a 200 mm width and the hybrid beam was fixed by belts to prevent it from scattering (Fig. 4).

The impact load and the displacement of the impactor were measured by load cells attached to both supporters and by a high-speed camera, respectively.

## 3. Numerical Analysis by FEM

### *3.1. FEM Model*

In the numerical analysis, a dynamic explicit FEM solver (PAM-CRASH Solver 2006) was employed. The FEM model was created based on the size of the specimens, impactor and the support parts in the experiment. The FEM model is shown in Fig. 5. The elastic–plastic shell element (MAT103) for the Al beam part and the unidirectional composite global ply shell element (MAT131, ITYP = 1) for the CFRP laminate were used, respectively. The impactor and the supporters were modeled as a rigid body. The mass of 100 kg and an initial velocity of 55 km/h were

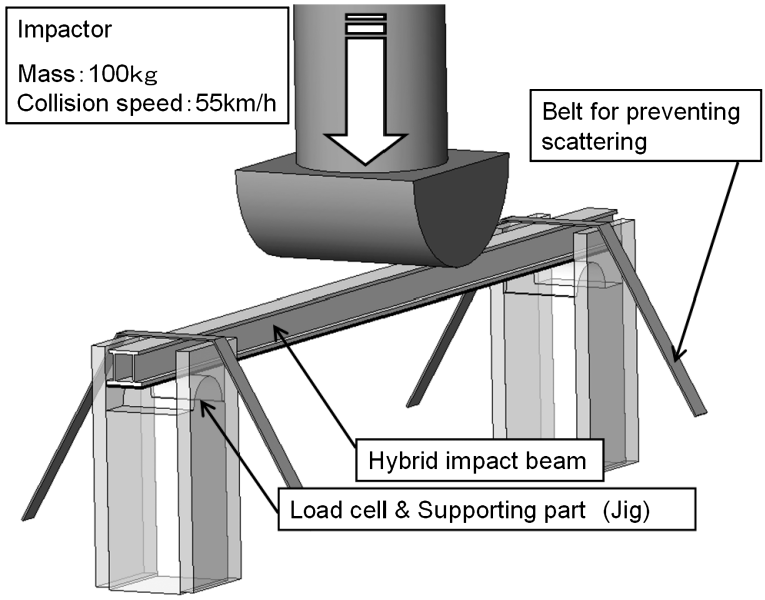


**Figure 4.** Outline of impact test.

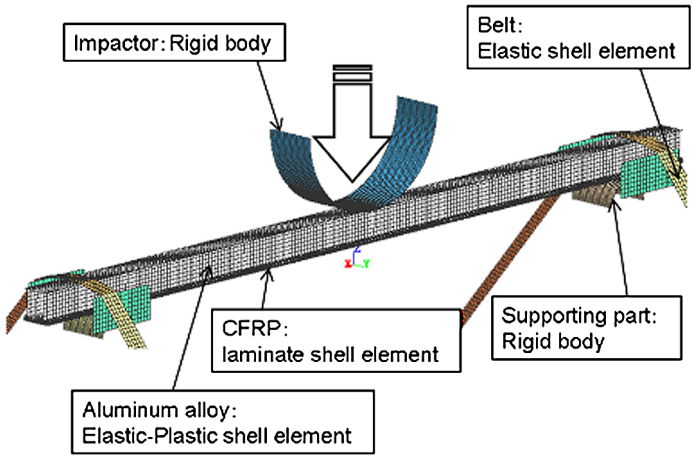


**Figure 5.** FEM analytical model. This figure is published in color on http://www.ingentaconnect.com/content/vsp/acm

given to the impactor. The total node number was 21 583 and the total element number was 19 504. The contact elements between the impactor and the upper surface of the hybrid CFRP/Al beam and between the supporter and the lower surface of the hybrid CFRP/Al beam were Contact Type 33 with the friction and penalty coefficients of 0.17 and of 0.1, respectively. The value of 0.1 is based on the empirical and not on the theoretical one which is recommended by the solver company to avoid noise and divergence in the numerical calculation. For the interface of the Al

**Table 1.**
Material properties of aluminum alloy

| Aluminum alloy | Tensile strength (MPa) | Yield stress (MPa) | Elastic modulus (GPa) | Poisson ratio |
|---|---|---|---|---|
| Z6W-T5 | 480 | 412 | 70 | 0.33 |

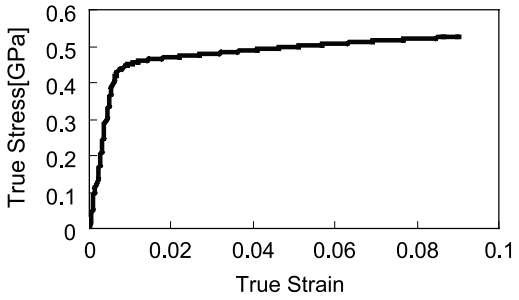


**Figure 6.** True strain–true stress curve of aluminum alloy.

**Table 2.**
Material properties of adhesive

| Type of adhesive | $\sigma_{max}$ (MPa) | $E$ (GPa) | $\tau_{max}$ (MPa) | $G$ (GPa) | $E_{frc}$ (kN/mm) | |
|---|---|---|---|---|---|---|
| | | | | | Model | Model |
| High strength | 30 | 3 | 25 | 1.15 | 0.006 | 0.005 |
| High elongation | 10 | 0.36 | 10 | 0.138 | 0.004 | 0.004 |
| Viscosity | 1 | $0.1 \times 10^{-4}$ | 1 | $0.038 \times 10^{-4}$ | 0.01 | 0.01 |

**Table 3.**
Material properties of CFRP

| CFRP | $F_L$ (MPa) | $E_L$ (GPa) | $F_T$ (MPa) | $E_T$ (GPa) | $F_{LT}$ (MPa) | $G_{LT}$ (GPa) | $V_{LT}$ |
|---|---|---|---|---|---|---|---|
| T700S, #2500 | 2550 | 135 | 69 | 8.5 | 98 | 4.4 | 0.34 |
| T800H, #3900-2B | 2840 | 160 | 80 | 7.8 | 98 | 4.4 | 0.34 |
| M40J, #2500 | 2450 | 230 | 53 | 7.7 | 59 | 3.9 | 0.27 |

beam and the CFRP laminate, 'Link Material 303' was used to model the adhesion of the interface.

Table 1 shows the material properties of the aluminum alloy and Fig. 6 shows its true strain–true stress curve. Table 2 shows the material properties of three kinds of adhesive and Table 3 shows the material properties of three kinds of CFRP.

For the failure criterion of the Al beam element, a 5% decrease of thickness in the tension state or a 30% increase of thickness in the compression state was used. Next, as the failure criteria of adhesive, 'Fracture energy of mode 1 and mode 2 of Link Material 303' was employed and a simple mode-independent maximum stress theory was used for the CFRP laminates. The fracture energy values $E_{\mathrm{frc}}$ of mode 1 and mode 2 are listed in Table 2. These values were calculated from the following equation:

$$E_{\mathrm{frc}} = \sigma_{\max} \text{ (or } \tau_{\max}) \cdot d_{\max}/2, \tag{1}$$

where $\sigma_{\max}$ and $\tau_{\max}$ are listed in Table 2 and $d_{\max}$ was the maximum displacement of adhesive layer between the CFRP and aluminum alloy. Its value was 0.4, 0.8 and 20 mm for the high strength, high elongation and the viscosity adhesives, respectively. When the value of the element was greater than these criteria, it was deleted in the succeeding FEM calculation.

### 3.2. Comparison of Experimental and FEM Results

Figure 7 shows the impact load to displacement relationship obtained by the experiment and the FEM for the No. 18 specimen, which absorbed the highest impact energy. In the experiment, after the impact load reached its maximum value of 24.0 kN and dropped to one-half value in the earlier time of impact, it soon recovered to almost the same value because of the effects of CFRP reinforcement. The center of the unidirectional CFRP laminate broke at the displacement of 126 mm and the impact load became zero at the displacement of 164 mm. The absorbed impact energy until the displacement of 150 mm was 1827 J. This value was somewhat higher or almost the same as that of the steel door guarder beam. The FEM result showed almost the same impact behavior and the absorbed impact energy obtained by the FEM was 1822 J and the error of impact energy was 0.27% compared with the experimental one. Figure 8 compares the failure mode of the hybrid beam and the two results showed the same breakage of CFRP laminate at the center of the hybrid beam.

In order to demonstrate the further effectiveness of the FEM method developed here by estimating another failure mode of the hybrid CFRP/Al beam, the result of

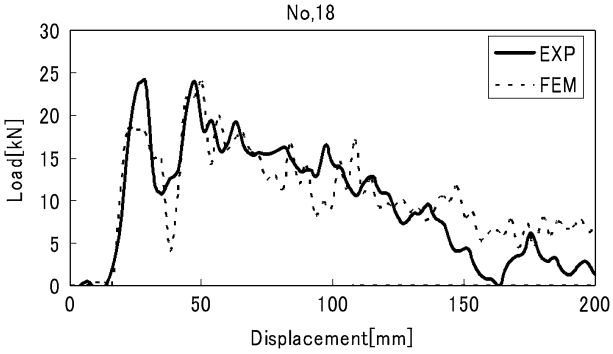


**Figure 7.** Comparison of experimental result with the FEM one (for specimen No. 18).

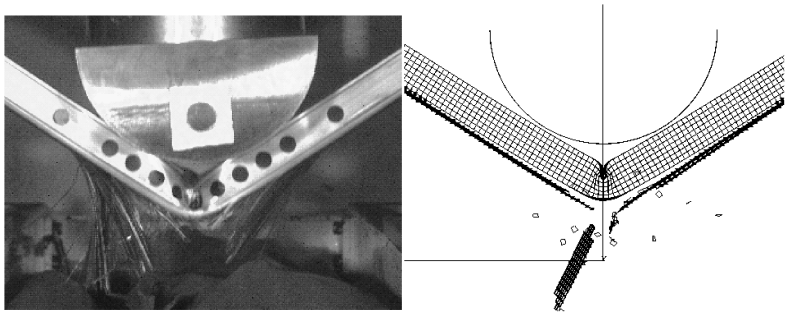

**Figure 8.** Comparison of experimental fracture mode with the FEM one (for specimen No. 18).

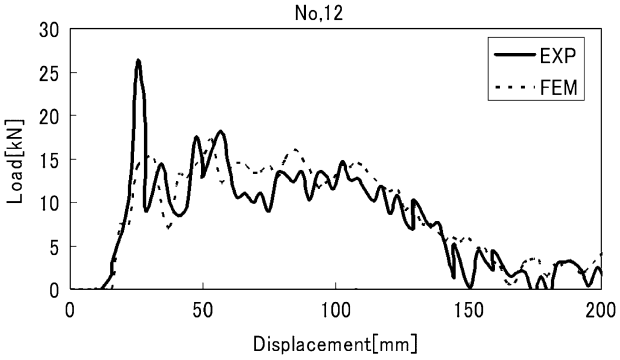


**Figure 9.** Comparison of experimental result with FEM one (for specimen No. 12).

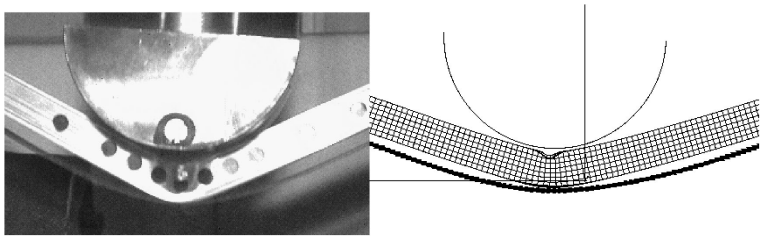

**Figure 10.** Comparison of experimental fracture mode with FEM one (for specimen No. 12).

No. 12 specimen, which showed the breakage of adhesive rather than the breakage of CFRP laminate, was compared with that obtained by the FEM. This specimen could not absorb the larger impact energy and its value was 1493 J. The reason for this was that the CFRP laminate came off the surface of Al beam because the breakage of adhesive occurred more rapidly than that of CFRP laminate. Figure 9 expresses a good agreement of the load–displacement relation except for the value of initial peak of load and the error of absorbed impact energy was 7% between both results.

Figure 10 shows the failure mode of the two results. The CFRP laminate came off the Al beam in both cases because of the breakage of adhesive. The failure mode of other specimens listed in Table 4 shows the mixture of both breakages of CFRP lam-

**Table 4.**
Impact energy absorption for all specimens

| No. | Type of CFRP | Thickness of CFRP (mm) | Width of CFRP (mm) | Type of adhesive | Break mode | Absorbed energy in experiment (J) | Absorbed energy in analysis (J) | Error (%) |
|---|---|---|---|---|---|---|---|---|
| 1 | T700S, #2500 | 1 | 36 | Viscosity | Fiber break | 1345 | 1384 | 2.90 |
| 2 | T700S, #2500 | 2 | 28 | High elongation | Fiber break | 1342 | 1358 | 1.19 |
| 3 | T700S, #2500 | 3 | 20 | High strength | Delamination | 1605 | 1685 | 4.98 |
| 4 | M40J, #2500 | 1 | 28 | High elongation | Fiber break | 1531 | 1529 | 0.13 |
| 5 | M40J, #2500 | 2 | 20 | High strength | – | – | – | – |
| 6 | M40J, #2500 | 3 | 36 | Viscosity | Fiber break | 1583 | 1574 | 0.59 |
| 7 | T800H, #3900-2B | 1 | 36 | High strength | Fiber break | 1626 | 1737 | 6.83 |
| 8 | T800H, #3900-2B | 2 | 28 | Viscosity | – | – | – | – |
| 9 | T800H, #3900-2B | 3 | 20 | High elongation | Delamination | 1371 | 1470 | 7.22 |
| 10 | T700S, #2500 | 1 | 20 | High elongation | Fiber break | 1549 | 1595 | 2.97 |
| 11 | T700S, #2500 | 2 | 36 | High strength | Fiber break | 1570 | 1627 | 3.63 |
| 12 | T700S, #2500 | 3 | 28 | Viscosity | Delamination | 1487 | 1591 | 6.99 |
| 13 | M40J, #2500 | 1 | 20 | Viscosity | Fiber break | 1322 | 1430 | 8.17 |
| 14 | M40J, #2500 | 2 | 36 | High elongation | Fiber break | 1815 | 1748 | 3.69 |
| 15 | M40J, #2500 | 3 | 28 | High strength | Fiber break | 1569 | 1663 | 5.99 |
| 16 | T800H, #3900-2B | 1 | 28 | High strength | Fiber break | 1667 | 1692 | 1.50 |
| 17 | T800H, #3900-2B | 2 | 20 | Viscosity | Delamination | 1636 | 1613 | 1.41 |
| 18 | T800H, #3900-2B | 3 | 36 | High elongation | Fiber break | 1827 | 1822 | 0.27 |

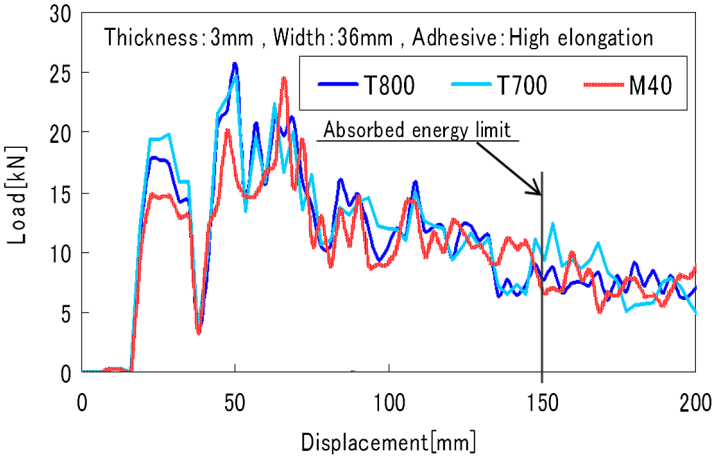


**Figure 11.** Displacement–load curves of three kinds of hybrid beams with different CFRP. This figure is published in color on http://www.ingentaconnect.com/content/vsp/acm

inate and adhesive. Table 4 also lists the impact energy absorption for all of the specimens except for the No. 5 and No. 8 specimens owing to a failure of the experiment.

The No. 18 specimen which absorbed the largest impact energy consisted of 3 mm thickness and 40 mm width of T800 and the high elongation adhesive. The average error of impact energy absorption for all the specimens was 3.65% between the experimental and the FEM results.

## 4. Increase of Impact Energy Absorption

### *4.1. Comparisons of Three Kinds of CFRP*

In the experiment, the No. 18 specimen using T800 CFRP absorbed the largest impact energy. However, the specimens whose only change was from T800 to T700 or M40 were not fabricated. In order to obtain the larger impact energy absorption, the two hybrid beams having the CFRP laminate of T700 or M40 were analyzed using the FEM method while maintaining other design parameters.

Figure 11 compares three results of specimens with T800, T700 and M40. The result from T700 showed the highest first peak of impact load and the largest impact energy absorption until the displacement reached 150 mm. Its value was 1863 J and an increase of 41 J was obtained compared with the case of T800.

Although the largest strength of CFRP is T800 and the largest Young's modulus of $E_L$ is M40 in Table 3, the result of T700 was the most proper CFRP among the three CFRPs. In hybrid beams made of CF/Al, neither high strength nor high Young moduli were required for the CFRP. Higher failure strains that follow the deformation of Al beams are the most important property for CFRP.

### *4.2. Design of Al Beam Cross-Sections*

Next, the cross-sectional shape of Al beam under the condition of keeping the same area was changed as a design parameter in order to increase the impact energy

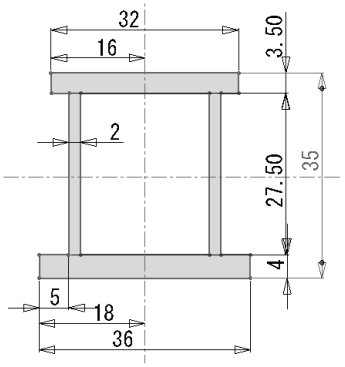


**Figure 12.** Cross-section of original beam.



absorption. Here, the thickness of 3 mm and the width of 36 mm of T700 CFRP and the adhesive of high elongation type were employed in the numerical simulation of FEM. The area of cross-section of Al beam used in the experiment (called the original section hereafter) was 366 $mm^2$, as shown in Fig. 12 and the four kinds of cross-sectional shape as shown in Fig. 13(a)–(d) were devised under the condition of keeping the same area as that of the original beam.

The vertical members of the cross-section in Fig. 13(a) were increased from 2 to 3 by reducing the thickness of the horizontal members and this was called the III beam. Figure 13(b) shows the higher vertical members compared with those of the original beam aiming at a larger second moment of area and it was called the II beam. In Fig. 13(c), the two vertical members crossed each other and this was called the X beam. Finally, one thicker vertical member was connected to the upper and the lower horizontal members (Fig. 13(d)) and this was denoted as the I beam.

The displacement–load curves of these four hybrid beams having the devised cross-section of Al beam were compared with that of the original hybrid beam in Fig. 14. Among them, the II section showed the highest impact load at the earlier time of impact and the III section presented the larger and constant impact load (about 20 kN) until the displacement of 120 mm.

The impact energies of absorption for the hybrid beams with the III, II and X sections were 2245 J, 2171 J and 2056 J, respectively. They were larger than 1822 J of the original hybrid beam except for the hybrid beam with the I section. The absorbed impact energy of the hybrid beam with the III section was 23% larger than that of the original one.

### *4.3. Comparison of Experimental and FEM Results for III Beam*

In the numerical calculations, the same calculation parameters in the same FEM stated before were used and their results were compared with those from the experiment executed after the calculation for confirming the effectiveness of the numerical method developed here. In order to confirm the performance of the III beam proposed in the FEM analysis, three prototypes (Fig. 15) of III beams were fabricated

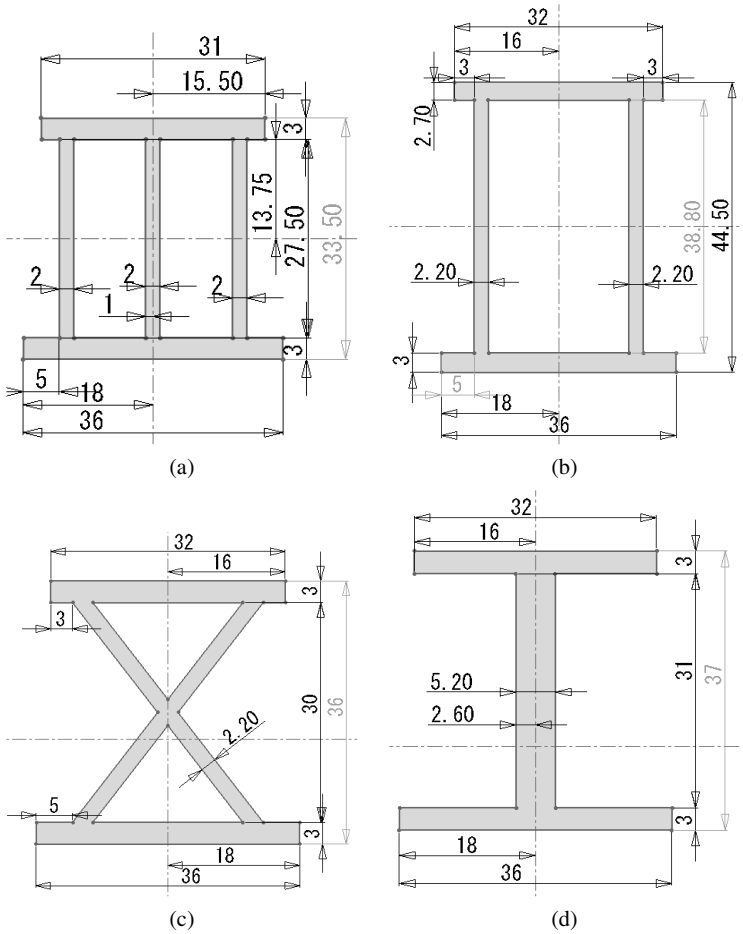


**Figure 13.** (a) Cross-section of III beam; (b) cross-section of II beam; (c) cross-section of X beam; (d) cross-section of I beam.

and their experiments were executed. Figure 16 shows the comparison of three experimental load–displacement curves with that of the FEM. The FEM curve showed the good agreement with three experimental curves and the average of experimental absorbed energy was 2119 J. The error between the experiment and the FEM was 5.6%. The impact energy absorption of the III beam was higher than the value from 1500 J to 1900 J in the conventional steel beam. Figure 17 shows the failure mode obtained from one of the specimens and the FEM and they also showed good agreement.

## 5. Methods of Installing a Hybrid Beam to Doors

### *5.1. Mechanical Method*

In order to install the hybrid beam to automotive doors, both ends of the No. 18 specimen, which obtained the highest impact energy absorption in the experiment,

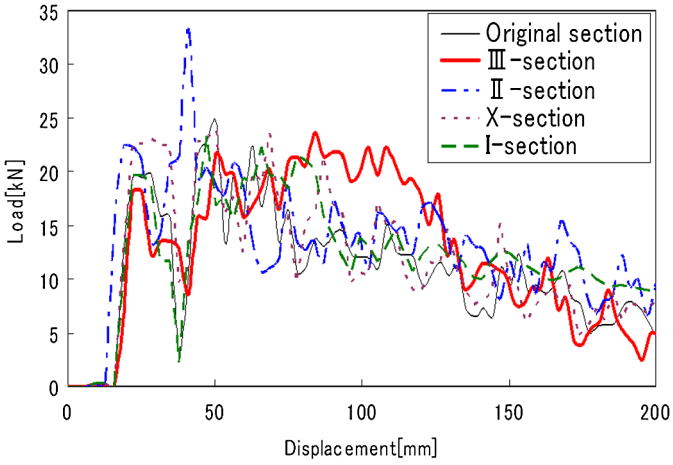


**Figure 14.** Comparisons of displacement–load curves for five hybrid beams. This figure is published in color on http://www.ingentaconnect.com/content/vsp/acm

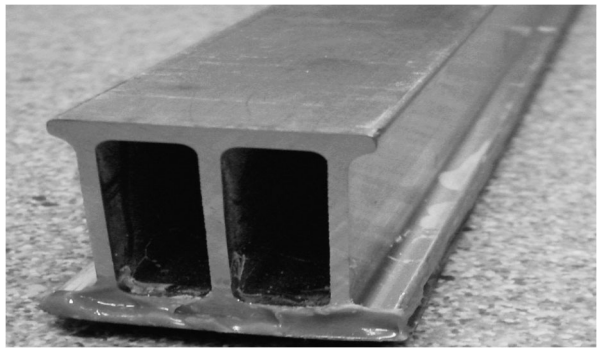

**Figure 15.** Prototype of III beam.

were cut slantingly and were connected to the door panel with bolts, as shown in Fig. 18. The impact energy absorption of the mechanical fastening method was calculated by the FEM analysis. In the FEM calculation, the door panel and the bolts were supposed not to fail before the failure of the hybrid beam.

Figure 19 shows the impact load–displacement curve of No. 18 hybrid beam with the mechanical joint. From this figure, the value of 3368 J was obtained as the impact energy absorption within the 150 mm displacement and this value seems to be the upper bound of impact energy absorption in the mechanical joint because the failure of the interface between the bolts and the hybrid beam is supposed to proceed before the failure of hybrid beam itself.

### *5.2. Adhesive Method*

In the adhesive method, the rectangular shape of socket with two ribs was used as shown in Fig. 20. The socket was made of Al alloy and its length and thickness

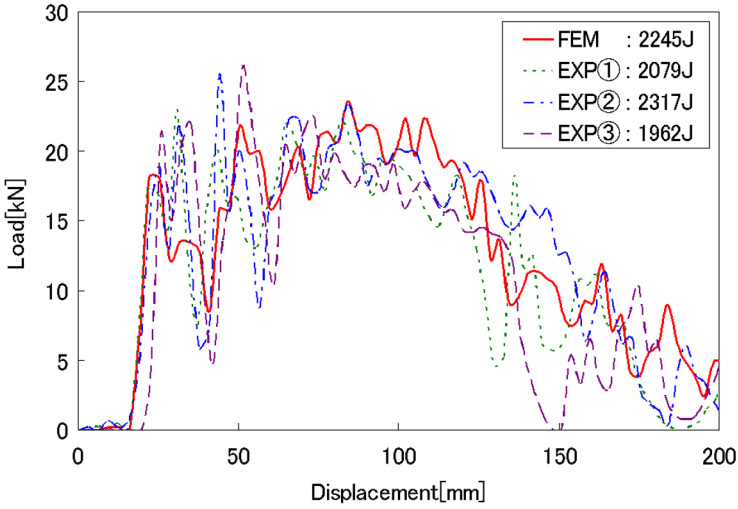


**Figure 16.** Comparison of experimental and FEM results for III beam. This figure is published in color on http://www.ingentaconnect.com/content/vsp/acm

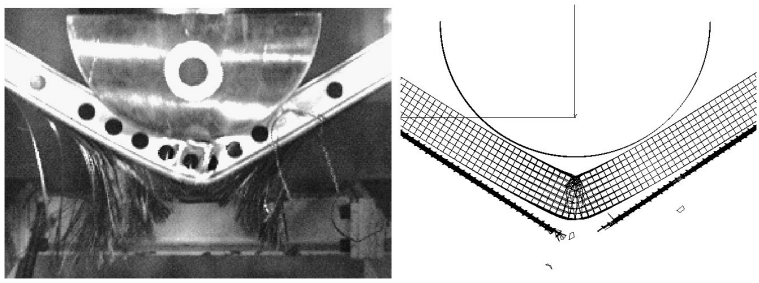

**Figure 17.** Comparison of fracture mode obtained both results.

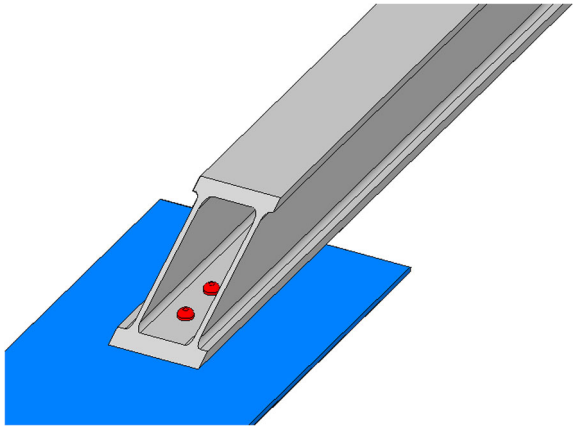

**Figure 18.** Mechanical joint of hybrid beam. This figure is published in color on http://www.ingentaconnect.com/content/vsp/acm

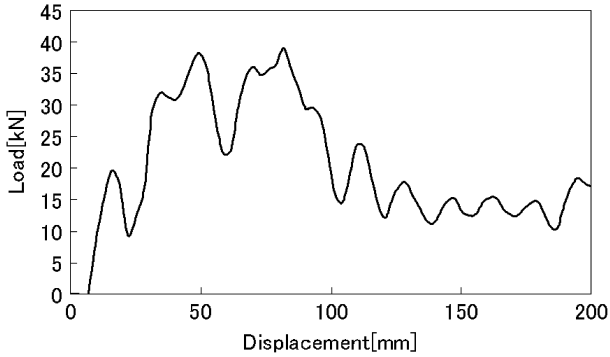


**Figure 19.** Load–displacement curve for mechanical joint.

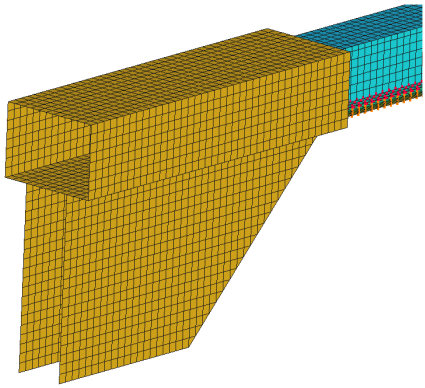

**Figure 20.** Adhesive method with two ribs. This figure is published in color on http://www.ingentaconnect.com/content/vsp/acm

were 200 mm and 2 mm, respectively. The 100 mm length of No. 18 hybrid beam was inserted into the socket and was bonded with high elongation adhesive.

Figure 21 shows the impact load to displacement curve for the No. 18 hybrid beam with the adhesive method. The dotted line shows the result in which the interface failure was introduced between the inner surface of socket and the inserted surface of No. 18 specimen and the impact energy absorption was 2951 J. On the other hand, the solid line shows the result in which the high elongation adhesive was supposed not to fail before the failure of the No. 18 hybrid specimen and the impact energy absorption of 4134 J was obtained as the upper bound value.

## 6. Conclusions

1. From the comparison of the FEM results with the experimental ones for specimens of CFRP/Al hybrid beams, the proposed numerical method was found to be very useful for calculating and simulating the impact behavior of hybrid beams.

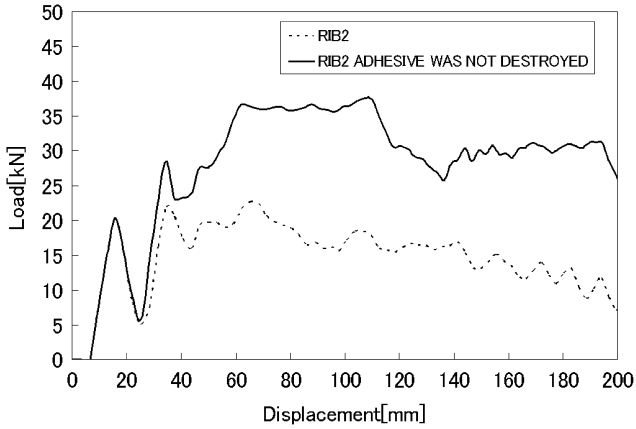


**Figure 21.** Load–displacement curve for adhesive joint.

2. The CFRP/Al hybrid door guarder beam showed an excellent performance of absorbing impact energy and its maximum value was larger than that of a steel beam. On the other hand, the maximum displacement of the hybrid beam after impact was smaller than that of a steel beam.
3. The CFRP/Al hybrid beam with the higher failure strain of CFRP showed the larger impact energy absorption because the CFRP could follow the failure of aluminum alloy beam.
4. The change of the cross-section of the Al beam increased the impact energy absorption and this fact was verified by the numerical simulation of FEM and three experimental results. Therefore, changing the design parameters of the hybrid beam may result in further increase of impact energy absorption.
5. The mechanical and adhesive methods of installing a hybrid beam onto automotive doors were concretely proposed and their impact absorption energy was considerably higher than that of conventional impact steel beams.



*Acknowledgements*

This study was conducted as part of the Japanese National Project R and D of Carbon Fiber Reinforced Composite Materials to Reduce Automobile Weight supported by NEDO (the New Energy and Industrial Technology Development Organization) and the authors acknowledge the assistance of Toray Co. and Nissan Automobile Co. who supplied the materials for these test specimens.

## References

1. P. K. Mallick and L. J. Broutman, Static and impact properties of laminated hybrid composites, *J. Testing Eval.* **5**, 190–200 (1977).

2. S. S. Cheon, T. S. Lim and D. G. Lee, Impact energy absorption characteristics of glass fiber hybrid composites, *Compos. Struct.* **46**, 267–278 (1999).
3. D. G. Lee, T. S. Lim and S. S. Cheon, Impact energy absorption characteristics of composite structures, *Compos. Struct.* **50**, 381–390 (2000).
4. G. Ben, T. Uzawa, H. S. Kim, Y. Aoki, H. Mitsuishi and A. Kitano, Impact strength and response behavior of CFRP thin belt, *Trans. JSME Series A* **70**, 824–829 (2004). (In Japanese.)
5. A. G. Caliskan, Axial and lateral impact prediction of composite structures using explicit finite element analysis, in: *Proc. IME2002, ASME Intl Mech. Engng Congress and Exposition*, New Orleans, USA (2002).
6. H. S. Kim, G. Ben and Y. Iizuka, Low-velocity impact behavior of CFRP-steel hybrid members, in: *Proc. 11th US-Japan Conf. Compos. Mater.*, Yonezawa, Japan (2004).
7. G. Ben, Y. Aoki and H. S. Kim, Comparison of experimental results with FEM for impact behaviors of Al door guarder beam reinforced with CFRP, in: *Proc. 12th US-Japan Conf. Compos. Mater.*, Dearborn, MI, USA (2006).
8. G. Ben, Y. Aoki and N. Sugimoto, Impact properties of CFRP/AL hybrid beam for absorbing impact energy, in: *Proc. 16th ICCM, FrFM-02*, Kyoto, Japan (2007).